ELSEVIER

Journal of Nuclear Materials 266–269 (1999) 642–647

journal of nuclear materials

The role of neutrals in the H–L back transition of high density single-null and double-null gas-fueled discharges in DIII-D

T.W. Petrie [a,*], R. Maingi [b], G.D. Porter [c], S.L. Allen [c], M.E. Fenstermacher [c], R.J. Groebner [a], D.N. Hill [c], A.W. Leonard [a], C.J. Lasnier [c], M.A. Mahdavi [a], R.A. Moyer [d], M.E. Rensink [c], D.M. Thomas [a], W.P. West [a], the DIII-D Team

[a] *General Atomics, P.O. Box 85608, San Diego, CA 92138-5608, USA*
[b] *Oak Ridge National Laboratory, USA*
[c] *Lawrence Livermore National Laboratory, USA*
[d] *University of California, San Diego, USA*

Abstract

The role of neutrals in triggering the H–L back transition in high density ELMing H-mode plasmas is explored in double-null (DN) and single-null (SN) divertors. We propose that the neutral particle buildup below the X-point may play an important role in triggering the H–L transition at high density. © 1999 Elsevier Science B.V. All rights reserved.

Keywords: Divertor; Density limit; Detachment; ELM_y H-mode

1. Introduction

The addition of cold deuterium gas into single-null (SN) ELMing H-mode diverted plasmas can trigger the formation of low-temperature ($\sim$ 1–2 eV), high density ($\gtrsim 2 \times 10^{20}$ m^{-3}), highly radiating region located between the X-point and the divertor floor [1–3]. Because the formation of this high density region has similarities with MARFE behavior [4], we refer to it as a 'divertor MARFE' and the conditions under which it occurs as the 'Partially Detached Divertor' (PDD) regime [3]. While some details may differ, other tokamaks, such as Alcator C-MOD [5], JET [6], and ASDEX-Upgrade [7] have reported similar observations. Continued gas puffing during SN PDD operation produces a transition back to the L-mode regime. This 'back transition' is characterized by a cessation of ELMing activity and a drop in edge plasma density.

While much of tokamak research currently is focused on plasma behavior in SNs, future generation tokamaks may require double-null (DN) divertor configurations to achieve 'high performance' characteristics, such as enhanced energy confinement and high plasma β. Some 'high performance' scenarios, moreover, may necessitate DN operation at densities where PDD conditions could exist, at least based on SN extrapolations. For this reason, the question of whether high density behavior in SNs can be used to predict high density behavior in DNs needs to be addressed. In this paper we examine this issue, particularly the role that the poloidal distribution of the neutral particles might play. After describing our basic experimental setup in Section 2, we detail the important characteristics of high density PDD SNs in Section 3 and contrast these with high density DNs in Section 4. In Section 5, we discuss our results.

2. Experimental setup

The SN and balanced DN plasma configurations discussed in this paper are representative of low triangular ($\delta_T \approx 0.4$) discharges with moderate separation of the X-point from the divertor tiles ($h_{X\text{-point}} \approx 0.12$ m). By 'balanced' we mean that the radial separation of the

* Corresponding author. Tel.: +1 619 455 4671; fax: +1 619 455 4156; e-mail: petrie@gav.gat.com.

PII: S0022-3115(98)00598-4

separatrices for the upper and lower divertor as projected back and measured at the outer midplane is $\leqslant 0.1$ cm. We focus on low triangularity configurations in both SN and DN for two main reasons. First, low triangularity SNs and DNs give the most favorable diagnostic coverage of the (lower) divertor plasma, especially with respect to measuring electron density and temperature (e.g., with the divertor Thomson scattering and Langmuir probe systems). Although no similar diagnostic capability exists in the upper divertor at present, an 'upper divertor' density and temperature can be 'measured', in a manner of speaking, with the lower divertor diagnostics by reversing the toroidal field (and, hence, the grad-B drift direction). The second reason to focus on the low-δ_T DN mode is that it allows comparisons with a large database of low triangularity SN divertor plasmas.

3. H–L transition in single-null divertors

Fig. 1 describes the evolution of an ELMing single-null H-mode plasma during cold deuterium (D_2) gas injection. The PDD was initiated at $t = 2.73$ s and the H–L backtransition occurred at $t = 3.32$ s. The latter is evidenced by a cessation of ELMing recycling activity and a drop in the 'edge' (pedestal) density ($n_{e,ped}$ in Fig. 1(b)). The PDD operating 'window' (i.e., between the initiation of the PDD and the H–L back transition) for the line-averaged electron density ($\bar{n}_e$ in Fig. 1(b)) was in the range $\bar{n}_e/n_{e,G} = 0.82$ to 0.98, where $n_{e,G}$ ($= I_p/\pi a^2$) is the Greenwald density limit [8]; typically, the width of this operating window for DIII-D plasmas is 0.1–0.2 in units of $\bar{n}_e/n_{e,G}$. The density profile was flat to modestly peaked during most of the PDD mode, since the electron density measurement deep in the core plasma ($n_{e,core}$) tracks $\bar{n}_e$ and $n_{e,ped}$ (Fig. 1(b)). The n_e-profile became more peaked near the H–L limit, however, when $n_{e,core}$ increased as $n_{e,ped}$ decreased. Energy confinement shortly before the H–L transition was roughly 40–50% lower than during pre-puff times; typically, $\tau_E/\tau_{E89\text{-}L} \approx 1.1$–1.3 immediately preceding the H–L transition as defined above, where $\tau_{E89\text{-}L}$ is the ITER89-L energy confinement [9].

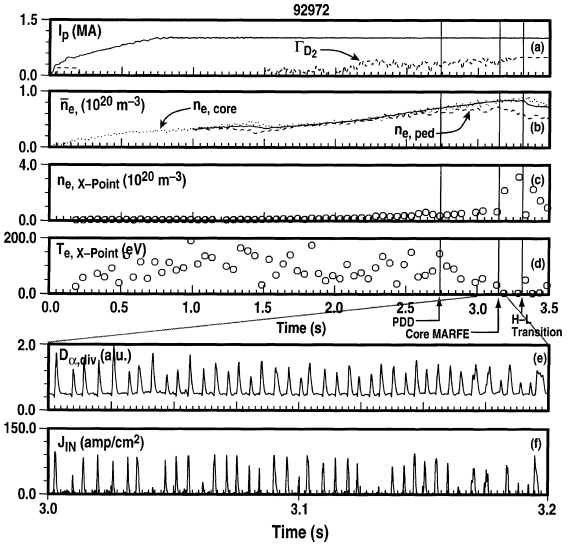

Fig. 1. Partially detached single-null divertor undergoes significant changes in both core and divertor behavior prior to the H–L transition: $B_T = 2.1$ T, $a = 0.61$ m, $q_{95} = 3$ 2. $D_{\alpha,div}$ indicates D_α recycling activity in the divertor, $\bar{n}_e$ is the line averaged density, $n_{e,ped}$ is the pedestal density, $n_{e,core}$ is electron density measured well inside the plasma core, $n_{e,X\text{-point}}$ and $T_{e,X\text{-point}}$ are electron density and temperature measured by Thomson scattering inside the core plasma near the separatrix and J_{in} is the saturation current under the inboard separatrix (Langmuir probes).

While total radiated power (P_{rad}) near the H–L density limit ~80% of the neutral beam power, bolometric inversions indicate that most of this radiation occurs *outside* the separatrix. The radiated power from inside the separatrix (i.e., the 'core' radiated power) is ≈15% of the input power for this shot; in general, the core radiated fraction is 15–30% near the H–L density limit for SNs. Carbon was the principal impurity radiator. Typically, the carbon concentration in the core plasma is approximately 1% during the ELMing PDD.

Neutral pressure measured in the private flux region shortly before the H–L back transitions depends strongly on both input power and toroidal field (i.e., $\propto P_{input}^2/B_T^2$). For the DIII-D SNs, neutral pressure in the private flux region is typically in the tens of milli-torr range prior to the H–L transition. For example, for SNs with similar parameters to the DNs we consider next ($P_{input} = 7$ MW, $B_T = 2$ T, and $I_p = 1.3$ MA), P_N prior to the H–L backtransition is ~40 mTorr).

There was significant electron density in the private flux region (e.g., ≈ 1–2 × 10^{20} m^{-3} during most of the PDD, where this density is measured half way between the X-point and the floor tiles directly under the X-

For SN plasmas with lower safety factors values (e.g., $q_{95} \leqslant 4.5$, as in this example), the back transition is preceded by the formation of a high density, low temperature region *inside* the separatrix near the X-point ('core MARFE'). This is indicated by the increase in electron density ($n_{e,X\text{-point}} > 2 \times 10^{20}$ m^{-3}) and a drop in electron temperature ($T_{e,X\text{-point}} < 5$ eV) *inside* the separatrix (core plasma) near the X-point (i.e., $t \approx 3.15$ s in Fig. 1(c),(d)). During the H-mode phases, the core MARFEs do not penetrate more than 5 cm above the X-point; this represents <1 cm from the plasma edge when traced along a field line back to the midplane. The appearance of the core MARFE is coincident with a decrease in both $n_{e,ped}$ and$\tau_E/\tau_{E89\text{-}L}$.

point). During normal PDD operation the inboard divertor leg is totally detached *between* ELM pulses. During ELMs, however, the inboard leg in SNs re-attaches, as shown by the jump in the saturation current under the inboard leg ($D_{\alpha,\mathrm{div}}$ and J_{in} in Fig. 1(e),(f)). This transient re-attachment of the inboard leg may contribute to the buildup of high neutral density in the private flux region (PFR) by both supplying the recycling particles and then preventing their escape from the PFR.

4. Single-null and double-null comparisons

4.1. The H–L density limit for SN and DN divertors

Data obtained during recent experiments with SNs [10] indicate that the H–L density limit has a dependence on toroidal field (i.e., $\sim(B_t)^{-0.5}$) and only a weak dependence on input power (i.e.,$(P_{\mathrm{input}})^{\varepsilon}$, where $\varepsilon \leqslant 0.1$). This scaling is different than the Greenwald density limit for L-mode plasmas, as there is no toroidal field dependence in Greenwald scaling. After normalizing the H–L density limit to B_{T} and P_{input} and 'windowing' on a common set of values for toroidal field, minor radius, and elongation, the H–L density limit in SNs increases roughly linearly with I_{p}. We find that the line-averaged density ($\bar{n}_{\mathrm{e}}$) for the DNs is ~15% higher than for the SNs. This translates into a higher average Greenwald fraction (i.e., $\bar{n}_{\mathrm{e}}/n_{\mathrm{e,G}}$, where $n_{\mathrm{e,G}}(10^{20}\,m^{-3}) = I_p(MA)/[\pi a(m)]^2$) for the DNs (i.e., ≈0.9) than for comparable SNs (i.e., $\lesssim 0.8$).

4.2. Global behavior of DNs at high density

Data from two high density, DN shots with opposite grad-B drift directions are plotted in Fig. 2. Both discharges were balanced during the times of interest. For later discussion of their divertor properties we have chosen a timeslice for each of these two shots at a common density value (i.e., $\bar{n}_{\mathrm{e}}/n_{\mathrm{eG}} \approx 0.95$, as in Fig. 2(b)).

At this density, $\tau_{\mathrm{E}}/\tau_{\mathrm{E89}}$ is ~1.6 for both shots. The rise in radiated power from the main plasma ($P_{\mathrm{rad,core}}$) largely accounts for this degradation in τ_{E} during the gas puffing phase (Fig. 2(c)). We observed higher radiated power in the divertor opposite the grad-B drift direction in the two timeslices selected. At these times the radiated power in the divertor/ X-point region opposite the grad-B drift direction was ~10–20% higher than the power radiated in the opposite divertor. Bolometric analysis has indicated that this divertor radiation was localized primarily along the outer leg of each divertor.

Neutral pressure in the private flux region (P_{N}) is <3 mtorr for the high density times considered (Fig. 2(d)) and are at least an order of magnitude lower than

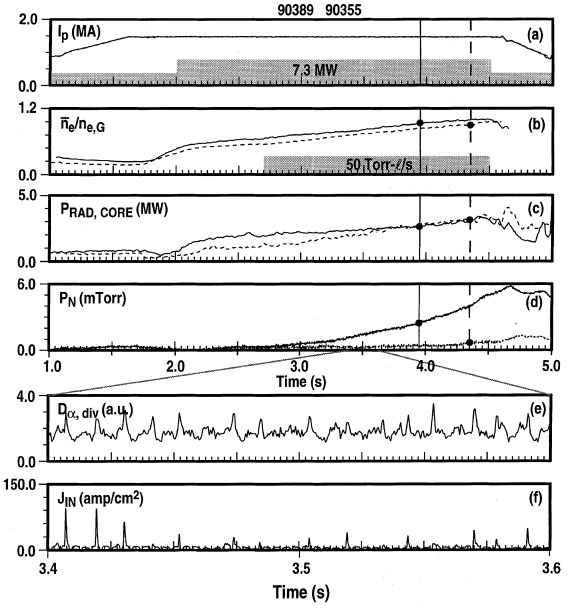

Fig. 2. Two high density ($\bar{n}_{\mathrm{e}}/n_{\mathrm{e,G}} = 0.95$) double-null discharges with opposite ∇B-drift directions shows some asymmetry in radiated power: ∇B-drift toward the upper divertor (solid) and ∇B-drift toward the lower divertor (dashed), $B_{\mathrm{T}} = 2.1$ T, $a = 0.61$ m, $q_{95} \simeq 4.5$. J_{in} is the saturation current near the inboard separatrix strike point from the shot with ∇B-drift toward the upper divertor.

comparable high density SN divertor discharges at a comparable $\bar{n}_{\mathrm{e}}$. As with SN PDD discharges at high density, the *inboard* legs of the DN divertor at high density are virtually detached between ELMs, that is, particle and heat fluxes under the inboard separatrix strike point decreased. With gas injection, the saturation current under the inboard legs showed significantly reduced activity, and a measurably reduced effect from ELMs on particle flux ($D_{\alpha,\mathrm{div}}$ and J_{in} in Fig. 2(e),(f)). This latter effect is in contrast to what we have observed in SNs.

4.3. Electron density and temperature in the divertor and at the X-point

It is instructive to take a closer look at the behavior of n_{e}, T_{e}, electron pressure (P_{e}) between the X-point and strike point along the outboard divertor separatrix for the $\bar{n}_{\mathrm{e}}/n_{\mathrm{e,G}} \approx 0.95$ cases above. There is no evidence of MARFE formation between the X-point and strike point (n_{e} in Fig. 3(a)); T_{e} along the separatrix was 'cold' (i.e., ≈3–4 eV) only near the strike point (Fig. 3(b)). That the electron temperature has cooled to <5 eV near the strike point, however, suggests that a divertor MARFE or 'partial detachment' may be near. There was a modest reduction in the electron pressure (P_{e})

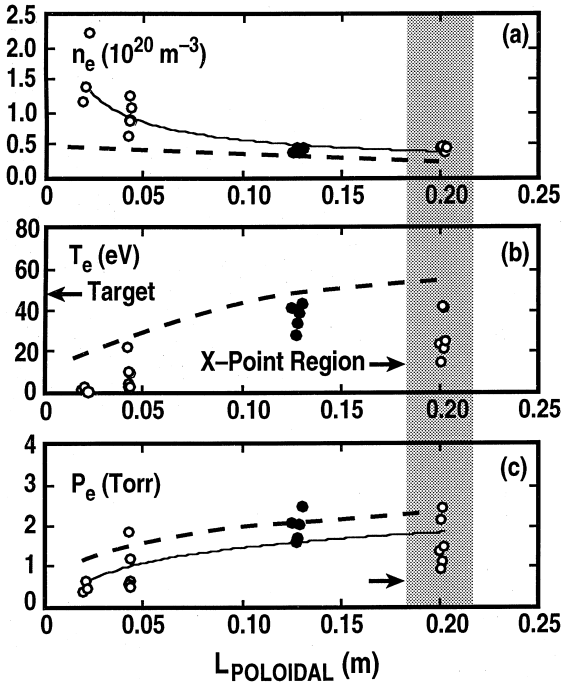

Fig. 3. A composite of the high density DN shots shown in Fig. 4 plots (a) electron density, (b) temperature, and (c) pressure versus poloidal length along the outboard separatrix between the X-point and strike point. The solid circles are data from the ∇B-drift toward the lower divertor; the open circles are data from the ∇B-drift toward the upper divertor. Data prior to gas puffing is represented by the dashed curves. PDD behavior is not observed.

along the separatrix between the X-point and the strike point (Fig. 3(c)); P_e between the X-point and the strike point for the DN prior to gas puffing is added for comparison (dashed line). For SNs during the PDD, the reduction in P_e during the PDD is typically higher (factor of ~6) [11].

The lack of a core MARFE at high densities (even near the H–L back transition) suggests that electron temperatures near either X-point (inside the separatrix) should be significantly higher than what one has found in SNs during high density (PDD) operation. The lack of a core MARFE is understandable from the measurement of T_e. For example, for the high density time slices in Fig. 2, the electron temperatures inside the separatrices at either of the X-points were still $\geqslant 50$ eV, well above temperatures where one might expect X-point MARFEs to form [11]. No evidence of a reduction of electron pressure *inside* the separatrix near either X-point during gas injection was observed. While n_e is higher and T_e is lower inside the separatrix for the $\bar{n}_e/n_{e,G} = 0.95$ timeslices than for similar measurements made in a non-puff case, we have found that the n_eT_e product is approximately the same for both non-puff and high density cases. In SNs, we have found that near the H–L transition T_e is often $\leqslant 20$ eV with core MARFEs frequently present.

4.4. Edge n_e and T_e

The edge (or 'pedestal') electron temperature ($T_{e,ped}$) has been suggested as an important ingredient in triggering the L–H transitions [12]. It has been further noted that the edge T_e at the H–L transition is approximately equal to the original edge T_e at the L–H transition [13]. Our data supports these contentions for the DN and SN cases examined. For example, the SN and DN plasmas in Fig. 4 had nearly identical I_p, P_{inj}, and B_T; Γ_{D2} for the DN was slightly higher, i.e., 120 versus 105 Torr l/s. Prior to gas injection, both discharges had type I 'giant' ELMs with frequency of 60–70 Hz and $\tau_E \cong 170$ ms. The L–H and the H–L transitions are indicated for each configuration. $T_{e,ped}$ for both cases underwent large excursions between their L–H and H–L transitions [Fig. 4(a)]. Yet, for both configurations, $T_{e,ped}$ was ap-

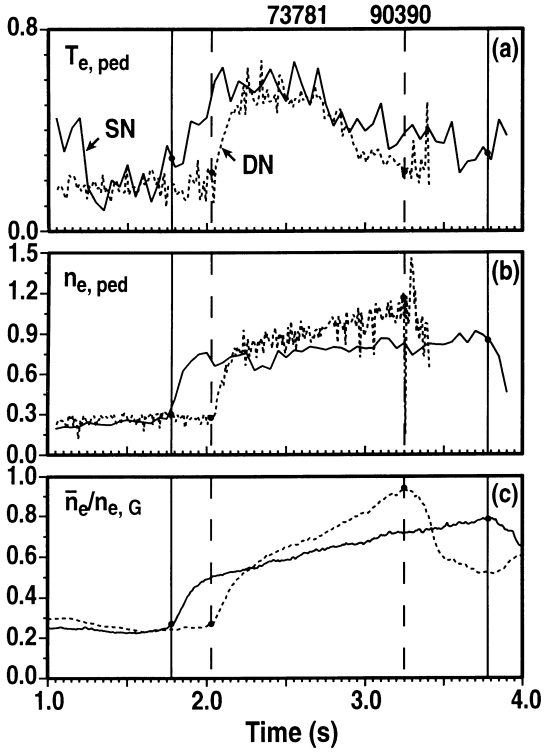

Fig. 4. (a) $T_{e,ped}$ at the L–H and H–L transitions are similar for both SN (solid) and DN (dashed) divertors. (b) $n_{e,ped}$ and (c)$\bar{n}_e/n_{e,G}$ increase significantly faster in the DN case during gas injection: $I_p = 1.5$ MA, $B_T = 2.1$ T, $\kappa = 2.0$, $q_{95} \simeq 4.5$, and $P_{inj} \simeq 7.2$ MW. Gas injection for the SN started at $t = 2.3$ s and for the DN at $t = 2.7$ s.

proximately the same at their respective L–H and H–L transition points. We have also compared the electron temperature profile near the plasma edge and found them to be virtually identical for the SN and DN cases near their H–L backtransition.

Pedestal electron density ($n_{e,ped}$), as expected, differed significantly at their respective L–H and H–L transition points (Fig. 4(b)). Note that both $n_{e,ped}$ and the normalized line-averaged density $\bar{n}_e/n_{e,G}$ (Fig. 4(c)) for the DN at the H–L backtransition were approximately 15–20% above those for the SN. Fig. 4(c) also shows that the density in the DN increased at over twice the rate in the SN. In general, DNs tend to fuel at a faster rate, as we discuss in Section 5.

5. Discussion

Fueling by gas puffing in DN configurations is more efficient than in SNs. This may be due to a combination of better direct ('first flight') fueling and improved access of the neutrals to the core plasma for the DNs. To show this is plausible, we use a simple particle balance model:

$$dN_i/d_t = S_{NBI} + \gamma S_{gas} - N_i/\tau_p \times (1 - R), \quad (1)$$

where N_i is the total ion particle content of the core plasma, S_{NBI} is the rate of beam particles ionizing inside the core plasma, S_{gas} is the gas puffing rate, γ is the fraction of gas puffed neutrals penetrating the core plasma directly from the gas injector, τ_p is the particle confinement time of the core plasma, and R is the fraction of recycled neutrals coming back into the core plasma after recycling.

We estimate N_i/τ_p for the cases described in Fig. 4 by first finding a self-consistent pair χ_{eff} and α, where χ_{eff} is the anomalous perpendicular diffusivity for thermal energy, $\alpha = 2.5\ D_\perp/\chi_{eff}$, and $D_\perp$ is the anomalous perpendicular diffusivity for particles. We follow Porter's approach [14], using the measured gradients in the density and temperature at the separatrix and the estimated power across the separatrix. We estimate γ computing the ionization mean free path for Franck–Condon neutrals (~3 eV), using the exponential scrapeoff n_e and T_e profiles from Thomson scattering and electron impact ionization data [15]. The results, shown in Table 1 suggest that roughly half of the improved fueling in DNs may be due to more efficient (direct) fueling and the other half may be due to the fact that a recycled neutral has a greater probability of re-entering the core (as opposed to being 'pumped' by the graphite tiles).

While the above global analysis is useful in identifying possible sources for improved fueling in DNs, it does not explain *why* R is higher in the DN. To address this issue, we need to understand why the SN and DN discharges near their (high density) H–L backtransitions behave so differently. The absence of the PDD during routine high density DN operation is especially noteworthy. Key to understanding this behavior is the realization that neutral pressure in the private flux region at either end of the DN divertor is much lower than in a corresponding SN at high density. Neutral particle pressure in the PFR has been identified as an important ingredient in triggering the PDD regime by transferring plasma momentum away from the divertor separatrix, possibly by charge-exchange or ion-neutral collisions [16,17]. Ghendrih [17], for example, has argued that this is applicable to DIII-D SN gas puffed discharges where the neutrals reduce plasma pressure along the divertor separatrix by charge-exchanging with ions, and has established a scaling for the neutral pressure needed for triggering the PDD. The neutral pressure measured in the PFR of (either) divertor in DN high density discharges is less than that required neutral pressure predicted by Ghendrih as necessary for triggering the PDD. From this perspective, it is understandable that the DNs did not reach the PDD regime.

Table 1
Particle balance: SN versus DN

	SN	DB
dN_i/dt (amps)	50	125
$S_{NBI\ (amps)}$	160	160
γ	0.045	0.065
$S_{gas\ (amps)}$	1100	1320
$N_i/\tau_p \times (1 - R)$ (amps)	160	121
R	0.800	0.865

Neutral pressure in the PFR is much lower in DNs than comparable SNs. The SN divertor has measurable density in the PFR during gas puffing (particularly during the PDD). It is more difficult for recycled neutrals to penetrate through this density barrier out of the divertor and into the core. This density barrier then inhibits fueling in SNs. In the DNs we have examined, we see no evidence of comparable density in the private flux region. Moreover, fewer neutrals accumulate in the divertor, due to better fueling in the DNs.

It is unclear as to why significant density forms in the private flux region of SNs but does not in DNs. We speculate that, while both SNs and DNs 'detach' along the inboard leg between ELMs (during gas puffing), ELMing events (briefly) re-attach the inboard leg. For SNs, continued gas puffing during the PDD resulted in an increase in ELM frequency and less time for the inboard leg to relax again to a detached state; hence, the ELMing pulse along the inboard leg helps build up neutral pressure in the PFR by both supplying recycling particles and then inhibiting their escape from the PFR through the inboard leg. On a qualitative level, ELMing events for DNs do not appear as 'strong' in terms of particle (or heat) flux as SNs. Partly responsible for this

may be that the particle and heat fluxes which flow to the high field side are divided between two poloidally separate locations in DNs, whereas these high field side flows are concentrated at a single poloidal location in SNs (i.e., 'sharing' by the divertors). In addition, if the particle flux from the ELMs (or even between-ELM contributions) are ejected primarily into the weak toroidal field side of the plasma as suggested by the time difference of an ELM pulse arriving at the inner and outer strike points [18], then the ELM pulse can be 'short-circuited' by either outboard divertor before it reaches the inboard divertors. We have measured the power flow to the outboard divertors and found it significantly greater than that to the inboard divertors (e.g., $\sim 6\times$ *before* D_2 injection). For SNs, this is $\sim 2\times$ [19].

6. Conclusion

We have shown that the road to the H–L back-transition for the single-null and double-null cases were very different, although their $T_{e,ped}$ (or T_e profile) were very similar at the back transition. We suspect that the detachment/reattachment of the inboard leg during ELMing conditions plays a pivotal role in the build-up of neutrals in the private flux region. Double-nulls are 'more detached' along their inboard legs than corresponding single-nulls. Thus, neutrals in the private flux region for double-nulls have a higher probability of escaping to the inboard side of the plasma and have direct fueling access to the core plasma. Spreading out the ionization of neutrals along the inboard plasma in double-null appears to lead to more efficient fueling of the core than allowing neutrals to accumulate in the divertor, as in single-nulls. Future work in understanding the high density behavior of single-null and double-null discharges should focus on the cause(s) of the in/out asymmetries in the particle and heat flux at the divertor targets, both during and between ELMing events.

Acknowledgements

Work supported by US Department of Energy under Contracts DE-AC03-89ER51114, W-7405-ENG-48, DE-AC05-96OR22464, and Grant No. DE-FG03-95ER54294.

References

[1] T.W. Petrie et al., Proceedings of the 18th Europ. Conf. on Controlled Fusion and Plasma Physics, Berlin, vol. 15C part III, 1991, p. 237.
[2] T.W. Petrie et al., J. Nucl. Mater. 196–198 (1992) 848.
[3] T.W. Petrie, Nucl. Fusion 37 (1997) 321.
[4] J. Drake, Phys. Fluids 30 (1987) 2429.
[5] B. Lipschultz et al., J. Nucl. Mater. 220–222 (1995) 50.
[6] G. Janeschitz et al., Proceedings of the 19th Europ. Conf. on Controlled Fusion and Plasma Physics, Innsbruck, vol. 16C part II, 1993, p. 727.
[7] M. Laux, Proceedings of the 20th Europ. Conf. on Controlled Fusion and Plasma Physics, Lisbon, vol. 17C part II, 1993.
[8] M. Greenwald, J. Terry, S. Wolfe et al., Nucl. Fusion 28 (1988) 2199.
[9] P.N. Yushmanov et al., Nucl. Fusion 30 (1990) 1999.
[10] T.W. Petrie et al., Behavior of double-null H–mode discharges at high density in DIII-D, in: 39th Annual Meeting of the Am. Phys. Soc., Div. of Plasma Phys., vol. 42, 1997, p. 1919.
[11] T.W. Petrie et al., J. Nucl. Mater. 241-–243 (1997) 639.
[12] ASDEX Team, Nucl. Fusion 29 (1989) 1959.
[13] H. Zohm et al., Fusion Energy 1996, Proceedings of the 16th International Conference Montreal, 1996, vol. 1, IAEA, Vienna, 1996, p. 439.
[14] G.D. Porter, Role of particle flow on power balance on DIII–D, Phys. Plasmas, submitted.
[15] R. Freeman, E. Jones, CLM-R-137, Culham Laboratory, Abingdon, 1977.
[16] P.C. Stangeby, Nucl. Fusion 33 (1993) 1695.
[17] Ph. Ghendrih et al., J. Nucl. Mater. 220–222 (1995) 305.
[18] D.N. Hill et al., Nucl. Fusion 28 (1988) 902.
[19] A.W. Leonard et al., J. Nucl. Mater. 220–222 (1995) 325.